Metal-Binding Characteristics of the Amino-Terminal Domain of ZntA: Binding of Lead Is Different Compared to Cadmium and Zinc†

Junbo Liu, Ann J. Stemmler, Juhi Fatima, and Bharati Mitra*

Department of Biochemistry and Molecular Biology, School of Medicine, Wayne State University, Detroit, Michigan 48201

Received November 8, 2004; Revised Manuscript Received February 8, 2005

ABSTRACT: ZntA from *Escherichia coli*, a P1-type ATPase, specifically transports Pb(II), Zn(II), and Cd(II). Most P1-type ATPases have an N-terminal domain that contains one or more copies of the conserved metal-binding motif, GXXCXXC. In ZntA, the N-terminal domain has ∼120 residues with a single GXXCXXC motif, as well as four additional cysteine residues as part of the CCCDGAC motif. The metal-binding specificity and affinity of this domain in ZntA was investigated. Isolated proteins, N1-ZntA and N2-ZntA, containing residues 1−111 and 47−111 of ZntA, respectively, were characterized. N1-ZntA has both the CCCDGAC and GXXCXXC motifs, while N2-ZntA has only the GXXCXXC motif. ICP-MS measurements showed that N1-ZntA can bind both divalent metal ions such as Cd(II), Pb(II), and Zn(II) and monovalent metal ions such as Ag(I), with a stoichiometry of 1. N2-ZntA can bind Zn(II) and Cd(II) with a stoichiometry of 1 but not Pb(II). The affinity of N1-ZntA for Zn(II), Pb(II), and Cd(II) was measured by competition titration with metallochromic indicators. Association constants of $\sim 10^8$ M^{-1} were obtained for Zn(II), Pb(II), and Cd(II) binding to N1-ZntA. To investigate whether the CCCDGAC sequence has an important role in binding specifically Pb(II), a mutant of ZntA, which lacked the first 46 residues, was constructed. This mutant, Δ46-ZntA, had the same activity as wtZntA with respect to Cd(II) and Zn(II). However, its activity with Pb(II) was similar to the mutant ΔN-ZntA, which lacks the entire N-terminal domain (Mitra, B., and Sharma, R. (2001) *Biochemistry 40*, 7694−7699). Thus, binding of Pb(II) appears to involve different ligands, and possibly geometry, compared to Cd(II) and Zn(II).

P1-type ATPases, also known as "heavy metal" and "CPx"-type ATPases, are a subgroup of P-type ATPases and catalyze the ATP-dependent transport of "soft"-metal ions across membranes (*1*−*3*). They play important roles in homeostasis of essential metals such as copper, cobalt, and zinc and mediate resistance to the highly toxic metals, cadmium, lead, and silver (*4*−*11*). ZntA from *Escherichia coli* confers resistance to toxic concentrations of cadmium, lead, and zinc by active efflux out of the cytoplasm (*4*, *5*). In humans, Menkes' and Wilson's diseases result from mutations in two copper transporting P1-type ATPases (*12*, *13*).

Most P1-type ATPases, both the monovalent and divalent metal-transporting ones, have a hydrophilic N-terminal segment containing one to six copies of a metal-binding motif, GXXCXXC; the Menkes' and Wilson's disease-associated proteins contain six copies each of this motif (*12*, *13*). In some copper pumps, the motif is histidine-rich (*9*). CoaT, the Co(II)-ATPase from *Synechocystis*, and its homologues are P1-type ATPases that lack an N-terminal metal-binding domain (*6*). The isolated N-terminal domains of both the Wilson's and Menkes' disease-associated proteins have been shown to bind a variety of metal ions, thus establishing this domain as a soft-metal binding module (*14*−*17*). An extended X-ray absorption fine structure (EXAFS) study of this domain from the Menkes' protein showed that one Cu(I) is bound for each CXXC motif and that Cu(I) binds to the two cysteine residues of this motif (*18*). The NMR structure of the fourth metal-binding repeat from the Menkes protein with Ag(I) bound supported this binding geometry (*19*).

The NMR structure of a portion of the N-terminal domain of ZntA, residues 46−118, has been solved; the overall protein structure was similar to the corresponding domain from the Cu(I)-ATPases (*20*). Zn(II) binds with tetrahedral coordination to the two cysteine and the aspartic acid residues of the GMDCAAC motif. The N-terminal domain of ZntA is distinct in that in addition to the GMDCAAC motif, four other cysteines are also present as part of the CCCDGAC sequence (Figure 1). This motif, CCX(D,E)XXC, is conserved in only a few close homologues of ZntA, notably those from *Salmonella typhi* and *Klebsiella pneumoniae*. The extra cysteines were not part of the Zn(II)-bound ZntA fragment the structure of which was solved by NMR, indicating that they are not required for binding Zn(II).

In this study, we characterized the metal-binding properties of the N-terminal domain of ZntA. The number of high-affinity metal binding sites in the isolated domain comprising residues 1−111 was determined to be one. The affinity of this domain for Zn(II), Pb(II), and Cd(II), the three substrate metals of ZntA, was determined by titration with two

† This work was supported by a United States Public Health Service Grant GM-61689 (to B.M.).

* Address correspondence to this author at Department of Biochemistry and Molecular Biology, Wayne State University School of Medicine, 540 E. Canfield Avenue, Detroit, MI 48201. E-mail: bmitra@med.wayne.edu. Phone: (313) 577-0040. Fax: (313) 577-2765.

10.1021/bi0476275 CCC: $30.25
Published on Web 03/11/2005

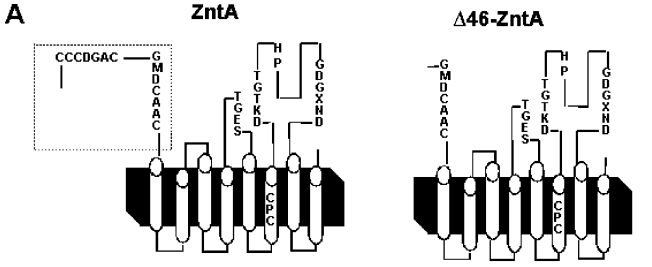

FIGURE 1: Panel A shows a schematic representation of ZntA and Δ46-ZntA. The N-terminus showing the two cysteine-rich motifs is enclosed in a dotted box. Panel B shows sequences of N1-ZntA and N2-ZntA, the isolated N-terminal domains of ZntA created in this study.

different metallochromic indicators; the affinity was quite high with association constants ranging from $\sim 10^7$ to 10^8 M^{-1}.

The role of the CCCDGAC sequence was investigated. Since the N-terminal domain bound only one metal ion, this sequence does not constitute a second tight metal-binding site. An isolated protein comprising residues 47−111 of ZntA, containing the GMDCAAC sequence, but lacking the CCCDGAC sequence, was characterized. It was unable to bind Pb(II), though Zn(II) and Cd(II) binding were unaffected. To confirm whether the CCCDGAC sequence plays a role in binding specifically Pb(II), we constructed a truncated mutant of ZntA, that lacks residues 2−46 and the CCCDGAC sequence (Figure 1). This protein, designated Δ46-ZntA,[1] behaves similarly to wtZntA with respect to both in vivo and in vitro activity with Cd(II) and Zn(II) as substrates. However, its activity with Pb(II) is similar to ΔN-ZntA, a mutant that we characterized earlier that lacks the entire N-terminal domain comprising residues 2−106 (*21*). Thus, the first 46 residues of ZntA, including the CCCDGAC sequence, play an important role in binding Pb(II) but not Cd(II) or Zn(II). Our results lead to the conclusion that the ligands and perhaps binding geometry of Pb(II) at the N-terminal metal site in ZntA are different from that of Zn(II) and Cd(II).

EXPERIMENTAL PROCEDURES

Materials. Plasmid pET-16b was from Novagen. Magfura-2 was from Molecular Probes. Chelex 100 (iminodiacetic acid agarose), 4-(2-pyridylazo)resorcinol) (PAR), and metal standard solutions were from Sigma. Standards for inductively coupled plasma mass spectrometry (ICP-MS) were from VWR. *E. coli* strain LMG194 was from Invitrogen, Carlsbad, CA.

Methods. Plasmids pET-N1-ZntA and pET-N2-ZntA. Two DNA fragments encoding amino acids 1−111 (N1-ZntA) and 47−111 (N2-ZntA) of ZntA were created by the polymerase chain reaction using the plasmid pZntA as a template and the oligonucleotides 5′-CTACTGTTTCTCCATACCC-3′ (P1) and 5′-CTGGGATCCTTACAGGGAATAGCCTGC-3′ (P2) for N1-ZntA, and 5′-ACGTCTCCATGGGCACCCGCTATAGC and P2 for N2-ZntA, respectively (Figure 1) (*21*). Both fragments contained a *Nco*I site at the 5′-end and a *Bam*HI site at the 3′-end. The two fragments were separately cloned into plasmid pET-16b using the *Nco*I and *Bam*HI sites to generate pET-N1-ZntA and pET-N2-ZntA.

Construction of pΔN-ZntA. The gene for the truncated mutant Δ46-ZntA, with residues 2−46 deleted, was generated by polymerase chain reaction methods using the oligonucleotides 5′-ACGTCTCCATGGGCACCCGCTATAGC-3′ and 5′-GAATTCTCTCCTGCGCAACAATCTTAACG-3′ together with the wild-type *zntA* gene as template. The resulting gene was cloned back into pBAD/*Myc*-His C, the same expression vector as for wtZntA, using the *Nco*I and *Eco*RI restriction sites to generate plasmid pΔ46-ZntA. As previously described, wtZntA was expressed as a carboxy-terminal hexahistidyl-tagged protein under control of the *araBAD* promoter (*22*). Δ46-ZntA was also expressed as a carboxy-terminal his-tagged protein.

Construction of the zntA-Deleted Strain, LMG194(zntA::cat). The *zntA* gene was fully deleted from the *E. coli* chromosome using the phage λ Red recombinase method (*23*). Plasmid pKD3 and strain BW25113 were kind gifts from Dr. Barry Wanner. The chloramphenicol resistance gene from pKD3, together with regions flanking the *zntA* gene, were amplified using the oligonucleotides 5′-TTCGGTTAATGAGAAAAAACTTAACCGGAGGATGCCGTGTAGGCTGGAGCTGGAGCTGC and 5′-GGGACCGATCGCGCTCAATGTTGCGATCGGTTTGCCCATATGAATATCCTCC. The PCR products were purified, digested with *Dpn*I, and electrotransformed into BW25113. Correct transformants were selected by screening on LB plates containing 25 μg/mL chloramphenicol.

The *zntA*-deletion was transferred to LMG194 by generalized transduction with P1 bacteriophage with selection for chloramphenicol resistance. The *zntA* deletion in LMG194-(*zntA::cat*) was finally confirmed by PCR using suitable oligonucleotides flanking the *zntA* gene.

All molecular biology experiments were performed according to established protocols. The sequences of N1-ZntA, N2-ZntA, and Δ46-ZntA were verified by automated DNA sequencing (Wayne State University, Detroit, Michigan). UV−visible spectra were recorded with a Varian (Cary 1E) spectrophotometer. Titration data were analyzed with the Kaleidagraph software.

Metal-Binding Specificity Using Metal-charged Chelex 100 Resin. The ability of the N-terminal domain of ZntA to bind different metal ions was tested using immobilized metal ion affinity chromatography. Chelex 100 was charged separately with Zn(II), Cd(II), Pb(II), Hg(II), Cu(II), Co(II), Ni(II), and Ag(I), and the proteins were then allowed to bind to the metal-charged resin. The bound proteins were eluted with EDTA and analyzed on SDS−PAGE.

Purification of N1-ZntA and N2-ZntA. BL21(DE3)pLysS cells, transformed with either pET-N1-ZntA or pET-N2-ZntA, were grown at 37 °C and induced with 0.1 mM IPTG. Harvested cells were stored at −70 °C. Frozen cells were resuspended in buffer A (50 mM 3-(*N*-morpholino)propanesulfonic acid (MOPS), pH 7.0, 2 mM EDTA, 5 mM

[1] Abbreviations: DTNB, 5,5′-dithiobis(2-nitrobenzoic acid); EDTA, ethylenediaminetetraacetic acid; N1-ZntA, a protein expressing residues 1−111 of ZntA; N2-ZntA, a protein expressing residues 47−111 of ZntA; Δ46-ZntA, a mutant of ZntA with residues 2−46 deleted; ΔN-ZntA, a mutant of ZntA with residues 2−106 deleted; PAR, 4-(2-pyridylazo)resorcinol; SDS−PAGE, sodium dodecyl sulfate polyacrylamide gel electrophoresis.

dithiothreitol (DTT), and 1 mM phenyl methyl sulfonyl fluoride (PMSF)), lysed, and centrifuged at 9000*g* for 30 min and 163 000*g* for 90 min. Following centrifugation, EDTA was removed from the supernatant by gel filtration on Sephadex G-25, and the lysate was loaded on a metal-charged Chelex 100 column. Chelex 100 was charged with zinc acetate or nickel chloride and equilibrated in buffer B (50 mM MOPS, pH 7.0, 2 mM DTT, 1 mM PMSF). The column was washed consecutively with buffer B, buffer B containing 250 mM NaCl, and buffer B containing 250 mM NaCl and 100 mM imidazole. The protein was finally eluted with buffer B containing 250 mM NaCl and 300 mM imidazole. The imidazole was removed by gel filtration on Sephadex G-25 equilibrated in buffer C (50 mM MOPS, pH 7.0, 50 mM KCl, 10% glycerol, 2 mM DTT, 1 mM PMSF). In some cases, an extra step was incorporated in the protocol before the Chelex-100 step. The protein was loaded on a DEAE-Sephacel column equilibrated in 20 mM 2-(*N*-morpholino)ethanesulfonic acid (MES), pH 6.0, containing 50 mM NaCl, 2 mM EDTA, 5 mM DTT, and 1 mM PMSF. Both N1-ZntA and N2-ZntA did not bind to this column under these conditions and could be purified to some extent by this step. The purified proteins were stored at − 70 °C. The purity of the proteins was checked by 13% sodium dodecyl sulfate polyacrylamide gel electrophoresis. The molecular weights of N1-ZntA and N2-ZntA were 11 814 and 7044 Da, respectively.

Determination of Protein Concentration for N1-ZntA and N2-ZntA. Protein concentrations were initially measured using a modified Lowry assay with the bicinchoninic acid reagent and bovine serum albumin as standard. However, given the necessity of obtaining accurate proteins concentrations for stoichiometry and binding affinity measurements, total amino acid hydrolysis was performed for both proteins (at W. M. Keck Foundation Biotechnology Resource Laboratories, Yale University). For N1-ZntA, the concentrations obtained from the Lowry assay and amino acid hydrolysis matched closely. However, for N2-ZntA, the Lowry assay overestimated the concentration by about ∼1.6-fold. Using the concentration obtained from amino acid hydrolysis, we calculated the extinction coefficient for N1-ZntA to be 1.14 $(mg/mL)^{-1}$ at 280 nm.

Measurement of Metal-Binding Stoichiometry to N1-ZntA and N2-ZntA Using ICP-MS. N1-ZntA and N2-ZntA were treated with 2 mM DTT and 5 mM EDTA at 4 °C for 1 h. DTT and EDTA were then removed by repeated cycles of dilution and concentration. Different metal salt solutions were incubated with the reduced apo-proteins for 1 h at 4 °C. For some experiments, the proteins were incubated with the metal salts in the presence of DTT. Excess metal salts (and DTT, when present) were removed either by passage over a Sephadex G-25 column or by dilution and concentration. Both methods yielded similar amounts of metal bound to protein within experimental error. Control protein samples were prepared in the same way, except metal salts were not added to the incubation mixture. Samples were prepared by digesting the required amount of protein with concentrated nitric acid at 70 °C for 1 h, then diluting with Nanopure water to 8 mL.

A PE Sciex Elan 9000 ICP-MS with a cross-flow nebulizer and Scott type spray chamber was used to measure metal concentrations. The RF power was 1000 W, and the argon flow was optimized at 0.92 L/min. The optimum lens voltage was centered on rhodium sensitivity. The data were collected as counts per second. A standard external calibration curve was determined from samples diluted from stock solutions of 1000 ppm standard solutions with appropriate buffer in 2% HNO_3 (high purity acid, OmniTrace@ EM Science). All of the reported ICP-MS data are the results of at least three replicate experiments performed for each of two to three different protein sample preparations.

Relative Affinity for Metal Measured Using Mag-fura-2 and PAR. The buffers and water used in these experiments were all passed through a Chelex 100 column to remove extraneous metal salts. The metal content of buffers after passing through a Chelex 100 column was estimated to be <50 nM. All buffers were deoxygenated and equilibrated with argon. Reduced apo-N1-ZntA was prepared by treating 1−2 mg of protein with 2 mM DTT and 5 mM EDTA at 4 °C for 1 h. DTT and EDTA were removed by passage through two consecutive Sephadex G-25 columns under argon flow. The reduced proteins were stored under anaerobic conditions. For competition titration with mag-fura-2, different aliquots of zinc chloride, lead acetate, or cadmium acetate were added using a gastight syringe to 10−20 μM apo-N1-ZntA and ∼20 μM mag-fura-2 in 10 mM Bis-Tris, pH 7.0, in a sealed cuvette under argon. An extinction coefficient of 29 900 M^{-1} cm^{-1} at 366 nm for metal-free mag-fura-2 was used to calculate the mag-fura-2 concentration (*24*). Binding of metal causes the spectrum to shift to an absorbance maximum of 325 nm. By monitoring the absorbance change at 366 nm, we could determine the concentration at which M(II) binds to mag-fura-2 and its stoichiometry and binding affinity for N1-ZntA.

For the competition titration with PAR, aliquots of reduced and anaerobic metal-free N1-ZntA were added from a gastight syringe to a mixture of 100 μM PAR and 20−40 μM zinc chloride in 10 mM Bis-Tris, pH 7.0, in a sealed cuvette under argon. Following each addition, the spectrum was recorded and corrected for dilution. The affinity of Zn(II) for N1-ZntA was calculated using an extinction coefficient of 66 000 M^{-1} cm^{-1} at 500 nm for the $Zn{\cdot}PAR_2$ complex (*25*).

Free Thiol Quantitation. The number of free thiols in native and denatured metal-free, reduced N1-ZntA and N2-ZntA was quantified using a standard DTNB assay (*26*). DTNB solution (final concentration 0.6 mM) was incubated with metal-free and reduced protein for 30 min in an anaerobic environment. The free thiolate concentration was calculated by measuring the absorbance at 412 nm (ϵ = 13 600 M^{-1} cm^{-1}). When the number of thiols in denatured proteins was estimated, the reaction with DTNB was carried out with proteins that were diluted in 400 μL of 6 M guanidine hydrochloride, pH 7.0.

Sensitivity to Soft Metal Salts. The sensitivity of LMG194, LMG194(*zntA*::*cat*), and LMG194(*zntA*::*cat*) transformed with either pZntA, pΔ46-ZntA, or pΔN-ZntA to metal salts was measured using a basal salts medium, pH 7.5, from which zinc salts were omitted (*27*). Cells were grown overnight and then diluted 50-fold in the same medium containing lead acetate, zinc chloride, or cadmium chloride. Cell growth at 37 °C was monitored by measuring the absorbance at 600 nm at fixed time intervals.

Table 1: Stoichiometry of Metal Binding to N1-ZntA and N2-ZntA Using ICP-MS[a]

	zinc	lead	cadmium	cobalt	copper	mercury	nickel	silver
N1-ZntA	1.1 ± 0.2	1.3 ± 0.1	1.0 ± 0.02	0.4 ± 0.03	1.1 ± 0.3	1.1 ± 0.3	1.1 ± 0.2	1.2 ± 0.1
N2-ZntA	0.9 ± 0.1	0.2 ± 0.04	1.0 ± 0.1	0.4 ± 0.06	1.1 ± 0.2	0.15 ± 0.1	0.1 ± 0.1	1.0 ± 0.1

[a] Metal bound and control samples were prepared as described in the Experimental Procedures. Typically, the metal content of control samples was <0.1% of the protein molar concentration (for Zn(II), control samples had <5% Zn(II) contamination). The reported values are averages of three independent protein and sample preparations.

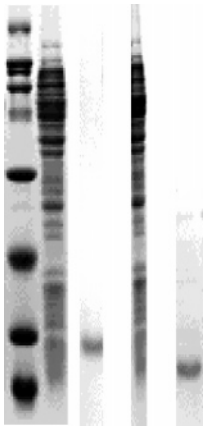

FIGURE 2: Purification of N1-ZntA and N2-ZntA analyzed by 13% SDS−PAGE stained with Coomasie Brilliant Blue. Lanes (from left to right) contain molecular weight markers, cell lysate containing N1-ZntA, purified N1-ZntA after metal−Chelex 100 column, cell lysate containing N2-ZntA, and N2-ZntA after metal−Chelex 100 column.

Purification and Assay of Δ46-ZntA. Δ46-ZntA was expressed by growing the pΔ46-ZntA-transformed LMG194-(*zntA*::*cat*) cells at 37 °C in Luria−Bertani medium followed by induction with 0.02% L-arabinose. The protein was purified using protocols used earlier for purifying ZntA and ΔN-ZntA (*21*, *22*). The purity of the proteins was checked by sodium dodecyl sulfate polyacrylamide gel electrophoresis. The metal ion-dependent ATPase activity was measured using a coupled assay with pyruvate kinase and lactate dehydrogenase. Purified protein was incubated with 1−2 mM dithiothreitol at 4 °C for 1 h prior to assays. The mixture contained 0.1 M acetic acid, 0.05 M BisTris and 0.05 M triethanolamine, pH 7.0, 0.1% purified asolectin, 0.1% Triton X-100, 10% glycerol, 5.0 mM each ATP and Mg(II), 0.25 mM NADH, 1.25 mM phosphoenolpyruvate, 14 units of pyruvate kinase, and 20 units of lactate dehydrogenase, with or without metal salts. Data were fitted to the Michaelis−Menten equation. Protein concentrations were determined using the bicinchoninic acid reagent with bovine serum albumin as standard.

RESULTS

Expression and Purification of N1-ZntA and N2-ZntA. The two fragments of the N-terminal portion of ZntA were expressed to different levels; N1-ZntA was more highly expressed compared to N2-ZntA. Both proteins could bind to Chelex 100 charged with most metals (data not shown). Utilizing this property in our purification protocol, we developed a scheme for purifying these fragments without any affinity tags. N1-ZntA was purified in a single step by binding to metal-charged Chelex 100. For N2-ZntA, we had to incorporate an additional DEAE-Sephacel step (Figure 2).

N2-ZntA contains only two cysteine residues, which are part of the conserved GMDCAAC motif, while N1-ZntA contains a total of six cysteines, including the four that are part of the CCCDGAC motif. As purified, the cysteines in both proteins were partially oxidized. The purified proteins were reduced with DTT and maintained under an argon atmosphere. When the number of free cysteines in the reduced proteins was measured using a DTNB assay, four free cysteines under native conditions and six under denaturing conditions were measured for N1-ZntA, as expected. Following 24 h of storage of the reduced proteins, the number of free cysteines in denatured N1-ZntA was still six, but in N2-ZntA it was typically less than 2. It appears that the cysteines of the CXXC motif are more susceptible to oxidation when the first 46 residues are removed from the N-terminal domain of ZntA; it is possible that these residues form a structure that prevents facile intermolecular oxidation of the cysteines in the CAAC sequence.

Stoichiometry of Metal Ion Binding to N1-ZntA and N2-ZntA Using ICP-MS. To understand the importance, if any, of the additional cysteine residues in the CCCDGAC motif, we determined the metal binding stoichiometry of N1-ZntA and N2-ZntA using ICP-MS. The results indicate that N1-ZntA binds only one metal ion with high-affinity; the additional cysteines, and the additional ∼46 residues, do not constitute a second high-affinity metal binding site in ZntA (Table 1). N1-ZntA could bind a variety of metals. The UV−vis spectrum of the copper-bound protein indicated that even though Cu(II) was incubated with the protein, the bound copper was in the Cu(I) form; there was no peak at wavelengths >600 nm, but a peak was present at 230−240 nm indicative of Cu(I)-thiolate charge-transfer complexes (data not shown). Therefore, the reduced N1-ZntA, when incubated with Cu(II) salts, reduces Cu(II) to Cu(I). The N-terminal domain of ZntA is thus capable of binding both monovalent (Cu(I) and Ag(I)) and divalent soft metal ions, though we have shown earlier that Ag(I) and Cu(I) are not substrates for the pump (*22*).

The stoichiometry of bound metal with N1-ZntA is 1 for all the metals except Co(II). We consistently obtained a stoichiometry of ∼0.5 for cobalt; moreover, the bound cobalt could not be displaced by Zn(II) or any other metal ions. The Co(II)-bound protein did not display the characteristic visible spectrum typical of Co(II)-thiolate charge-transfer complexes. These results suggest that the geometry and ligands of bound Co(II) are different from that of the other metal ions; also, one cobalt ion likely bridges two N1-ZntA monomers.

**The result of metal binding to N2-ZntA, which lacks the additional CCCDGAC motif, is quite interesting (Table 1). Like N1-ZntA, it also binds Zn(II), Cd(II), Cu(II), and Ag(I) with a stoichiometry of 1 and Co(II) with a stoichiometry of 0.5. However, unlike N1-ZntA, the stoichiometry obtained with Pb(II), Hg(II), and Ni(II) was 0.1−0.2. Therefore, removal of the first 46 residues, including the

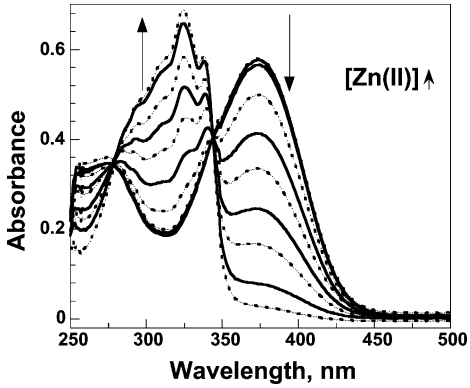

FIGURE 3: Representative spectra obtained during titration of 20 μM mag-fura-2 and 9 μM N1-ZntA with increasing concentrations of Zn(II) (0−40 μM) in 10 mM Bis-Tris, pH 7.0, at 20 °C. The arrows denote the direction of the absorbance changes as increasing concentrations of zinc chloride are added.

CCCDGAC motif, disrupts binding of these metals with high affinity. It is especially interesting that N2-ZntA is unable to bind Pb(II), which is the best substrate for ZntA (*22*). These results suggested that the extra domain in the N-terminus of ZntA plays a role in sensing and tight binding of specifically Pb(II). It is unclear why N2-ZntA is unable to bind Hg(II), since Hg(II) can bind in a linear coordination to the CXXC motif in proteins such as MerP. It is possible that the cysteines in the CXXC motif in ZntA are not optimally situated for a linear coordination geometry, given that this motif in ZntA has evolved to accommodate a tetrahedral binding geometry for Zn(II) and Cd(II). When both the CCCDGAC and the CXXC motifs are present as in N1-ZntA, Hg(II) may bind to cysteines from both these motifs.

It is to be noted that the experiments with ICP-MS were not performed under equilibrium binding conditions; rather, they were designed to measure the number of high-affinity metal binding sites. This is a reasonable approach, given that metals such as Zn(II) and Cd(II) are present at extremely low concentration inside the cells; moreover they are mostly bound to high-affinity sites on proteins and small molecule chaperones.

Affinity of Zn(II), Pb(II), and Cd(II) for N1-ZntA Using Metallochromic Indicators. The affinity of N1-ZntA for Zn(II), Pb(II), and Cd(II) was determined by competition titration with a metal indicator, mag-fura-2. Mag-fura-2 forms a 1:1 complex with these metals; the absorbance maximum changes from 366 nm in metal-free mag-fura-2 to 325 nm in the metal-bound form. To measure the affinity of N1-ZntA for metals, a mixture of mag-fura-2 and N1-ZntA was titrated with aliquots of metal salts; the decrease in absorbance at 366 nm as the metal-bound form increased in concentration was measured. Figure 3 shows the changes in mag-fura-2 upon binding Zn(II) in the presence of N1-ZntA. Figure 4A,B,C shows the plot of absorbance changes at 366 nm as a function of added Zn(II), Pb(II), and Cd(II) concentrations, respectively. The data were best fitted to eq 1, which describes a single binding site for M(II) on N1-ZntA. Attempts to fit the data to an equation with two metal binding sites resulted in a poor fit. This indicates that even under equilibrium conditions, N1-ZntA has a single tight metal binding site. The affinity of N1-ZntA for metal was calculated using eqs 2 and 3.

$$\text{N1-ZntA} + \text{M(II)} \leftrightarrow \text{N1-ZntA}\cdot\text{M(II)} \quad (1)$$

$$K_I = \frac{[\text{I}\cdot\text{M(II)}]}{[\text{I}_{(\text{free})}][\text{M(II)}_{(\text{free})}]} \quad (2)$$

$$K_N = \frac{[\text{N1-ZntA}\cdot\text{M(II)}]}{[\text{N1-ZntA}_{(\text{free})}][\text{M(II)}_{(\text{free})}]} \quad (3)$$

where K_I is association constant of the indicator, mag-fura-2, and M(II), [I·M(II)] and [$I_{(free)}$] are concentrations of the mag-fura-2 complex with M(II) and free mag-fura-2, respectively, obtained from the absorbance at 366 nm following each addition of M(II) and the initial concentration of mag-fura-2, [$M(II)_{(free)}$] is the free M(II) concentration calculated from eq 2, K_N is the association constant of N1-ZntA and M(II), and [N1-ZntA·M(II)] and [$N1\text{-}ZntA_{(free)}$] are the concentrations of the N1-ZntA complex with M(II) and free N1-ZntA, respectively, calculated from the total concentrations of N1-ZntA and M(II) using eq 2.

The value of K_I, the association constant of mag-fura-2 and Zn(II), was previously determined by fluorescence methods at 37 °C in 20 mM *N*-2-hydroxyethylpiperazine-*N*′-2-ethanesulfonic acid (HEPES), pH 7.4, containing 140 mM NaCl, to be 5×10^7 M^{-1} (*28*). We determined the association constants of Zn(II), Pb(II), and Cd(II) with mag-fura-2 by absorbance measurements to be 8×10^6, 6×10^5, and 3×10^7 M^{-1}, respectively, in 10 mM BisTris, pH 7.0,

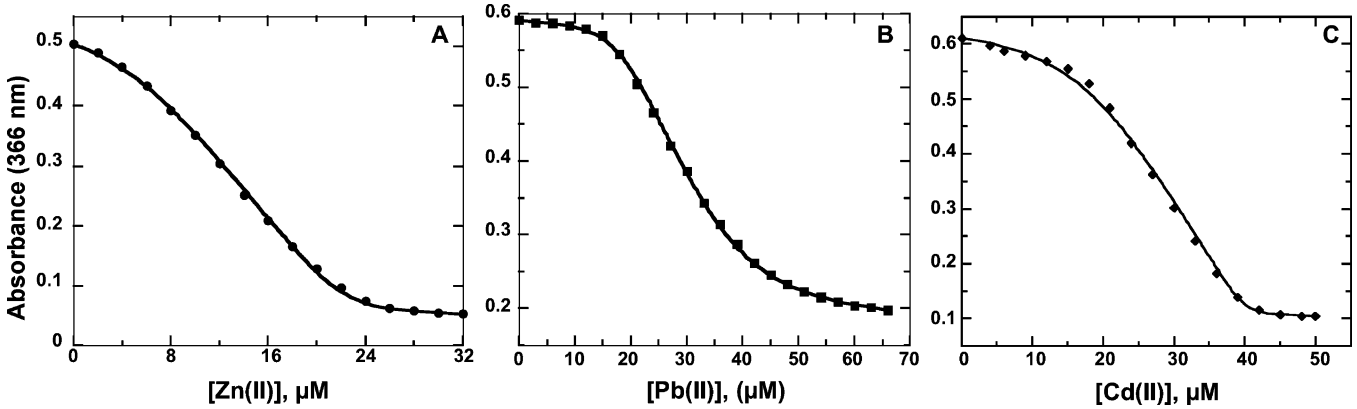

FIGURE 4: Plot of the absorbance changes at 366 nm when increasing concentrations of metal salt solutions were added to mag-fura-2 and N1-ZntA in 10 mM Bis-Tris, pH 7.0, at 20 °C: (A) Zn(II) with 6 μM N1-ZntA and 16 μM mag-fura-2; (B) Pb(II) with 18 μM N1-ZntA and 20 μM mag-fura-2; (C) Cd(II) with 18 μM N1-ZntA and 20 μM mag-fura-2. Data were fitted to eqs 2 and 3.

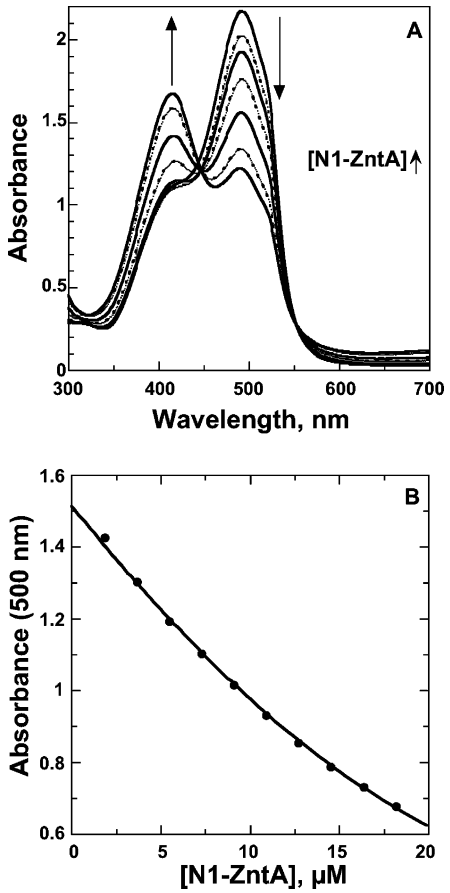

FIGURE 5: Panel A shows spectra obtained during titration of 100 μM PAR and 40 μM Zn(II) with increasing concentrations of N1-ZntA (0−30 μM) in 10 mM Bis-Tris, pH 7.0, at 20 °C. The arrows denote the direction of the absorbance changes as increasing amounts of N1-ZntA are added. Panel B shows titration of 100 μM PAR and 20 μM Zn(II) with increasing concentrations of N1-ZntA. Data were fitted to eq 5.

at room temperature. These values of K_I were used in eqs 1 and 2; in some cases, K_I was also varied during the data fitting. Using either the fitted value or the experimentally determined values for K_I, we obtained association constants, K_N, of $(4.8 \pm 0.7) \times 10^7$, $(2.1 \pm 0.5) \times 10^7$, and $(2.0 \pm 0.2) \times 10^8$ M^{-1}, respectively, for N1-ZntA binding to Zn(II), Pb(II), and Cd(II) in 10 mM BisTris, pH 7.0, at room temperature. Thus, the affinities of N1-ZntA for its three substrate metal ions are similar; also, these affinities are of similar orders of magnitude as that of mag-fura-2 for metal ions.

We also measured the association constant of N1-ZntA for Zn(II) using an indicator with an affinity for metal that is many orders of magnitude different from that of mag-fura-2. PAR is an indicator that forms both 1:1 and 2:1 complexes with Zn(II). The stepwise association constants for the formation of the Zn·PAR and Zn·PAR_2 complexes are 4×10^6 and 5×10^5 M^{-1}, respectively (*25*); thus the combined association constant of the Zn·PAR_2 complex, β_{PAR}, is 2×10^{12} M^{-2}. However, significantly higher association constants have also been reported for PAR (*29*). The affinity of N1-ZntA for Zn(II) was calculated by monitoring the decrease in absorbance at 500 nm as N1-ZntA displaced Zn(II) from the Zn·PAR_2 complex (Figure 5A). Equation 4 assumes a single Zn(II) binding site on N1-ZntA. Equation 5 was used to fit the data (Figure 5B).

$$\text{N1-ZntA} + \text{Zn·PAR}_2 = \text{N1-ZntA·Zn(II)} + 2\text{PAR} \quad (4)$$

$$\frac{K_N}{\beta_{PAR}} = \frac{[\text{N1-ZntA·Zn(II)}][\text{PAR}_{(free)}]^2}{[\text{N1-ZntA}_{(free)}][\text{Zn(II)·PAR}_2]} \quad (5)$$

The free PAR concentration was calculated from the absorbance at 500 nm using an extinction coefficient of 66 000 M^{-1} cm^{-1} following each addition of N1-ZntA. However, we could only obtain a lower limit for the association constant of Zn(II) with N1-ZntA accurately using this fit, since β_{PAR} is many orders of magnitude higher than K_N. Using PAR as an indicator, we obtained an association constant of N1-ZntA and Zn(II) that is $\geq (4.4 \pm 0.2) \times 10^7$ M^{-1} in 10 mM BisTris, pH 7.0. This value is quite similar to the more accurate value obtained using mag-fura-2 as an indicator.

The Resistance Profile of Δ46-ZntA with Respect to Pb(II), Zn(II), and Cd(II). Since the results with N1-ZntA and N2-ZntA indicated that deletion of the first 46 amino acids from the N-terminus affects the binding of Pb(II), we constructed a mutant of ZntA that lacks the first 46 amino acids and thus the CCCDGAC motif. The plasmid bearing the mutant gene, pΔ46-ZntA, was cloned into an *E. coli* strain from which the entire *zntA* gene was deleted. Figure 6 shows time courses of growth of a wild-type *E. coli* strain, LMG194, the *zntA*-deleted strain, LMG194(*zntA*::*cat*), and the deleted strain transformed with plasmids containing either a copy of the *wtzntA* gene or the *Δ46-zntA* gene. For comparison, we also included the deletion strain carrying a plasmid containing the *ΔN-zntA* gene, in which the first 106 residues of the N-terminal domain are deleted (*21*). All five strains grow well when toxic levels of Pb(II), Zn(II), and Cd(II) salts are absent in the growth medium (Figure 6A). However, when challenged with 10 μM Pb(II), 50 μM Zn(II), or 5 μM Cd(II), strain LMG194 was able to grow well, while the deletion strain, LMG194(*zntA*::*cat*), did not grow at all. The deletion strain transformed with pZntA was also able to grow, though a distinct lag of 5−7 h was observed (Figure 6B−D). On the other hand, the strain containing ΔN-ZntA, lacking both the CCCDGAC and GMDCAAC motifs, displayed quite different behavior. Growth was much slower and linear instead of logarithmic, after the initial lag. Though the strain was able to grow well after 24−30 h, it was clearly at a disadvantage relative to wtZntA with respect to resistance against these three toxic metals. We previously reported growth studies for a *zntA* disrupted strain, LMG194 (*zntA*::*kan*), carrying plasmids pZntA and pΔN-ZntA (*21*). In that study, we monitored growth after 24 h and reported that there was no difference between the behavior of wtZntA and ΔN-ZntA. The more rigorous studies reported in this work with a deletion strain show that while cell density after 24−30 h for ΔN-ZntA is similar to that of wtZntA, the strain carrying ΔN-ZntA has a definite lag compared to wtZntA for toxic levels of all three metal salts, Pb(II), Cd(II), and Zn(II).

The behavior of the deletion strain carrying Δ46-ZntA was most interesting. The growth in this case followed an identical pattern to that of wtZntA with respect to 50 μM Zn(II) and 5 μM Cd(II) in the growth medium but was similar to that of ΔN-ZntA with respect to 10 μM Pb(II) in the growth medium. Thus, growth was linear and slower than that of wtZntA when challenged with Pb(II) but not with Zn(II) and Cd(II).

Table 2: Kinetic Parameters Obtained for Δ46-ZntA at 37 °C for the Metal Ions Pb(II), Zn(II), and Cd(II) in the Absence and Presence of the Thiolate Form of Cysteine Present at a Concentration Equal to the Soft Metal Ion Concentration[a]

	ZntA[b]		Δ46-ZntA		ΔN-ZntA[c]	
	V_{max}	apparent K_m	V_{max}	apparent K_m	V_{max}	apparent K_m
Pb(II)	584 ± 30	4.8 ± 0.9	360 ± 14	6.1 ± 0.9	319 ± 6	11.6 ± 0.8
Zn(II)	247 ± 13	10.3 ± 1.9	250 ± 10	7.5 ± 1.0	81 ± 7	9.3 ± 1.2
Cd(II)	57 ± 3	5.5 ± 1.2	72 ± 4	5.5 ± 1.0	66 ± 3	4.1 ± 0.6
Pb(II) + thiolate	2500 ± 70	166 ± 15	1011 ± 59	42 ± 10	1095 ± 67	55 ± 11
Zn(II) + thiolate	710 ± 28	96 ± 11	766 ± 27	55 ± 7.5	372 ± 6	42 ± 3
Cd(II) + thiolate	1025 ± 25	252 ± 16	1164 ± 70	107 ± 21	388 ± 10	52 ± 5

[a] The assay buffer was 0.1 M acetic acid, 0.05 M BisTris, and 0.05 M triethanolamine, pH 7.0. The Mg(II) and ATP concentrations were 5 mM each. For comparison, data for ZntA and ΔN-ZntA are also included. V_{max} values are in nmol/(mg·min) and K_m values are in μM. [b] From ref *22*. [c] From ref *21*.

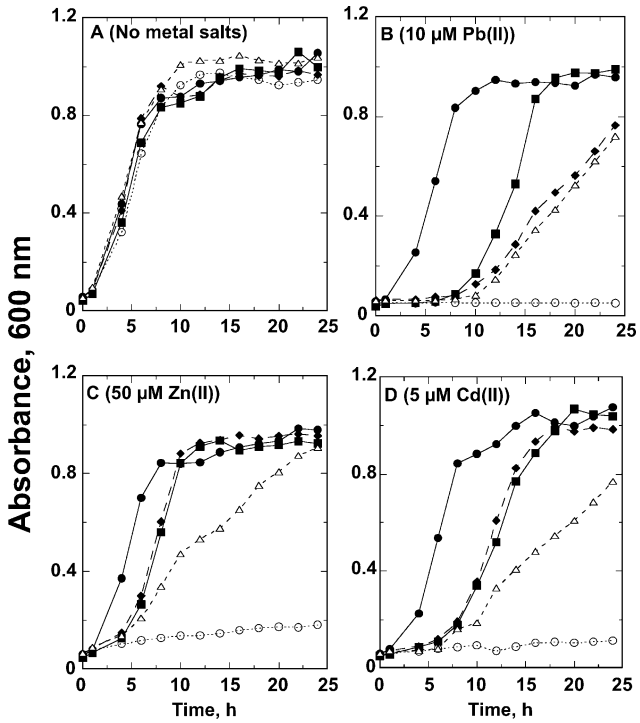

FIGURE 6: Resistance to Pb(II), Zn(II), and Cd(II) salts by the wild-type strain, LMG194 (●), the *zntA*-deleted strain LMG194(*zntA*::*cat*) (○), and the deleted strain transformed with the plasmids pZntA (■), pΔ46-ZntA(◆), and pΔN-ZntA (△). Cells were grown in a low phosphate medium in the (A) absence of any metal salts and in the presence of (B) 10 μM lead(II) acetate, (C) 50 μM zinc(II) chloride, and (D) 5 μM cadmium(II) chloride at 37 °C. Cell growth was monitored at the indicated time intervals by measuring the absorbance at 600 nm.

ATPase Activity of Δ46-ZntA. Δ46-ZntA was expressed using the same expression vector used for ZntA and ΔN-ZntA and purified using Ni(II)-affinity chromatography as described earlier for ZntA and ΔN-ZntA (*21*, *22*). We showed earlier that both ZntA and ΔN-ZntA show ATP hydrolysis activity that is significantly stimulated by Pb(II), Zn(II), or Cd(II) salts (*22*). Table 2 summarizes the kinetic parameters for Δ46-ZntA for the metal-stimulated ATPase activity at pH 7.0 and 37 °C; the data for ZntA and ΔN-ZntA are also included. The V_{max} for the Pb(II)-stimulated activity for Δ46-ZntA was ~360 nmol/(mg·min), lower compared to ~580 nmol/(mg·min) for ZntA; the apparent K_m for Pb(II) was similar. However, the V_{max} for the Zn(II)- and Cd(II)-stimulated activity was similar for Δ46-ZntA and ZntA. It should be noted that the K_m values for the soft metals in the absence of thiolates reported in Table 1 are apparent K_ms, since the metal ions are expected to exist as complexes with ATP.

The thiolate form of cysteine in the assay buffer increased the ATPase activity of Δ46-ZntA, just as we observed earlier for ZntA, though the apparent K_ms of the metals are much higher (Table 2) (*22*). The thiolate form of cysteine was added at a soft-metal ion/thiolate ratio of 1:1. In the presence of thiolates, Δ46-ZntA displayed a V_{max} value for Pb(II) that was similar to that of ΔN-ZntA and 2.5-fold lower than that of ZntA. However, the V_{max} values for Zn(II) and Cd(II) were similar for Δ46-ZntA and ZntA, and 2−3-fold higher than that of ΔN-ZntA. As expected, the apparent K_ms for all three metal ions were higher in the presence of thiolates for all three proteins. The activity profile clearly shows that Δ46-ZntA resembles wtZntA with respect to Zn(II) and Cd(II); however, as far as Pb(II) is concerned, its behavior is similar to ΔN-ZntA.

DISCUSSION

Most P1-type ATPases have a distinctive N-terminal domain containing metal binding motifs involving either cysteine or histidine residues. The highly conserved GXX-CXXC motif, found in both Cu(I) and Pb(II)/Zn(II)/Cd(II)-transporting ATPases, is also found in many other metal binding and redox-active proteins. Most Cu(I)-ATPases contain multiple copies of this motif and can bind more than one metal. In addition to a single copy of this motif, ZntA also contains the CCCDGAC sequence in its N-terminal domain. Metal-binding stoichiometry to two different constructs of the N-terminal domain of ZntA, N1-ZntA containing both the GMDCAAC and the CCCDGAC motifs and N2-ZntA containing only the GMDCAAC motif, clearly showed that only a single metal is bound to N1-ZntA with high affinity. Thus, either the CCCDGAC motif does not constitute a second metal binding site, or, two metal ions cannot be bound to these two motifs simultaneously due to steric constraints. The net result is the same; ZntA can only bind a single metal ion in its N-terminal domain with high affinity. It is possible that there is a second weak metal-binding site in N1-ZntA. However, given the extremely low concentrations of Zn(II), Cd(II), and Pb(II) in cells, it is unlikely that a weak metal binding site is physiologically relevant.

N1-ZntA can bind a wide variety of metal ions, both monovalent and divalent, as revealed by ICP-MS measurements. It can bind Ag(I), which is not a substrate of ZntA, either in vivo or in vitro (*4*, *22*). Similar observations were made for the Wilson's Cu(I)-transporting ATPase; its N-

terminal domain bound both the substrate Cu(I) and the nonsubstrate Zn(II), Cd(II), and other divalent ions, though with different binding geometry (*14*, *15*, *17*). A second interesting observation is that when Cu(II) binds to N1-ZntA, it is reduced to Cu(I). This was also observed for the Wilson's Cu(I)-ATPase; when Cu(II) was incubated with the N-terminal domain, the bound form was Cu(I) (*15*). This is consistent with the observation that though Cu(I)-transporting ATPases have an N-terminal domain that contains one or more copies of the CXXC motif, Cu(II)-containing ATPases have a histidine-rich N-terminal domain; it appears that the CXXC motif is not suitable for binding the Cu(II) ion (*30*). We also observed that binding of Co(II) to N1-ZntA was substoichiometric. It appears as if one Co(II) bridged two protein molecules in a configuration in which it could not be displaced by the substrate metals, Zn(II), Pb(II), or Cd-(II). This observation suggests that the CXXC motif is not optimally suited for binding Co(II) and may explain why Co(II)-ATPases lack a metal-binding N-terminal domain altogether (*6*, *30*).

Though the extra cysteines of the CCCDGAC motif do not constitute a second metal-binding site, the ICP-MS results suggested that they play a role in conferring specificity toward Pb(II). ZntA has the highest activity with Pb(II), and it is thus expected that the N-terminal domain of ZntA should be able to bind Pb(II) tightly. Therefore, it was surprising that removal of the CCCDGAC motif results in N2-ZntA not being able to bind Pb(II), Ni(II), and Hg(II) with high affinity. Since the structure of the 46−118 residue fragment of ZntA, which is similar in length to N2-ZntA, showed that it is a properly folded protein, it seemed unlikely that the lack of binding of Pb(II) to N2-ZntA was because it was misfolded (*20*).

To investigate this further, we compared the Δ46-ZntA mutant to ΔN-ZntA and wtZntA. In vivo, the Δ46-ZntA mutant behaves similarly to wtZntA as far as resistance to Zn(II) and Cd(II) is concerned, but its growth profile resembles that of ΔN-ZntA for resistance against Pb(II). In other words, as far as mediating resistance against Pb(II), deleting the first 46 amino acids has the same effect as deleting the first 106 amino acids. Activity assays of the purified protein support this conclusion. The only difference between Δ46-ZntA and wtZntA is that the V_{max} with Pb(II) is 2.5-fold lower, while the activity with Zn(II) and Cd(II) is unchanged for Δ46-ZntA. Thus, Pb(II) no longer shows the highest activity with Δ46-ZntA, unlike ZntA.

The N-terminal metal-binding domain in ZntA is clearly not required for in vitro activity or for metal specificity since both ΔN-ZntA and Δ46-ZntA are active. However, both the in vivo and in vitro results confirm that this domain confers a kinetic advantage to the transporter, which may be crucial in vivo. Our hypothesis is that the N-terminal metal-binding site is more solvent-exposed and binds metals more efficiently than the transmembrane metal-binding site. After binding metal ion, the N-terminal site passes it to the transmembrane site. In the absence of the N-terminal site, the transmembrane metal site is able to bind metal ions directly, but the process is kinetically less efficient. The results reported here suggest that the GMDCAAC motif in ZntA is sufficient to bind Zn(II) and Cd(II) efficiently. But the CCCDGAC motif is necessary to bind Pb(II); it confers high-affinity Pb(II) binding capability to a Zn(II)/Cd(II)-transporter. It is evident that Pb(II) binds to different ligands and perhaps with a different geometry relative to Zn(II) and Cd(II) to the N-terminal domain of ZntA. ZntA has the highest activity with Pb(II) in vitro (*22*). It is possible that this additional domain is conserved in those organisms, *E. coli*, *Salmonella*, and *Klebsiella*, for which the high levels of resistance to Pb(II) are crucial for survival.

The affinity of the N-terminal domain of ZntA for metal ions is an important parameter in understanding how metal ion transporters play a central role in determining free metal ion concentrations inside the cell. A major goal in this work was to determine the affinity of the N-terminal domain of ZntA for the substrate metals, Zn(II), Pb(II), and Cd(II), using competition titration with metallochromic indicators. In studies of this kind, it is important to select an indicator the affinity of which for metal is of similar magnitude to the affinity of the protein for metal; otherwise erroneously high affinities can be the result. Since we had no idea initially how tightly the N-terminal domain of ZntA bound metal ions, we chose two well-known Zn(II) indicators with widely different affinity for Zn(II), mag-fura-2 and PAR. The association constants of N1-ZntA for Zn(II), Pb(II), and Cd-(II) are $\sim 10^7-10^8$ M^{-1} with Cd(II) binding with slightly higher affinity than Zn(II) and Pb(II). These affinities were found to be in the same range as those of mag-fura-2 for these metals. Hence, we are confident that these values are accurate. PAR is an indicator typically used to measure the Zn(II) affinity of peptides in the $\sim 10^{12}$ M^{-1} range. Given the much lower affinity of N1-ZntA for Zn(II), we could not obtain an accurate affinity constant for N1-ZntA using PAR, only a lower limit. However, this limit, $\sim 5 \times 10^7$ M^{-1}, is in the same range as the values obtained with mag-fura-2.

Recently, the affinity of the N-terminal domain of Ccc2, the yeast Cu(I)-transporting ATPase, for Cu(I) was reported to be on the order of 10^{-19} M for the dissociation constant (*31*). This is a much higher affinity for Cu(I) than that of N1-ZntA for Zn(II), Cd(II), and Pb(II). It should be noted however, that Ccc2 is a transporter that imports Cu(I) from the cytoplasm into the Golgi, while ZntA is a pump that exports metal ions from the *E. coli* cytoplasm only when they reach toxic levels. The concentration of free Cu(I) inside the cell is expected to be lower than that of nonredox active metals such as Zn(II), Cd(II), and Pb(II) by many orders of magnitude. Also, an efflux pump like ZntA that transports Zn(II), Cd(II), and Pb(II) out of the cell would be expected to have metal affinity much lower than a transporter that pumps essential Cu(I) into the Gogi; otherwise, Zn(II) that is required in the cell would be pumped out by ZntA.

It is, of course, possible that the affinity of the N-terminal metal binding site for Zn(II), Pb(II), and Cd(II) may be modified when it is part of the full-length ZntA, as opposed to the isolated N-terminal domain, N1-ZntA. However, given the modular structure of P1-type ATPases, we believe that this is not the case, though this possibility will be examined in the future. The physiological function of ZntA is to pump out Zn(II) when concentrations reach toxic levels. Based on the affinity of N1-ZntA for Zn(II), Pb(II), and Cd(II) and the typical *E. coli* inner cell volume ($\sim 10^{-15}$ L), we can estimate that the N-terminal domain of ZntA is half-saturated with these metals when there are 1−10 free zinc, lead, and cadmium atoms in the cell. Current studies in our laboratory indicate that the affinity of the transmembrane metal binding site in ZntA for Zn(II) is of similar magnitude to that of

N1-ZntA for Zn(II) (J. Liu and B. Mitra, unpublished observation). Thus, it is likely that the function of the N-terminal metal-binding site in ZntA is to bind metal from solution or from chaperones and transfer it to the metal site in the membrane for subsequent transport.

Conclusion. In this work, we show that the N-terminal domain of ZntA has a single high-affinity metal-binding site; it binds both monovalent and divalent soft metal ions. When the first 46 amino acids containing an extra four cysteine residues are deleted, the isolated fragment, which still has the signature P1-type ATPase metal-binding motif, GXX-CXXC, can bind Cd(II) and Zn(II) but not Pb(II). The CXXC motif is not suitable for binding the cupric form of copper or Co(II). To confirm whether the Pb(II)-binding site in ZntA has contributions from the first 46 residues including the CCCDGAC motif, we characterized a mutant, Δ46-ZntA, which lacks the first 46 residues. Δ46-ZntA resembles wtZntA with respect to Zn(II) and Cd(II) for both in vivo resistance activity and in vitro ATPase activity. However, with respect to Pb(II), it behaves similarly to ΔN-ZntA, a mutant lacking the entire N-terminal domain. Thus the first 46 residues including the CCCDGAC motif are only important for the activity toward Pb(II). This suggests that Pb(II) binds to different ligands and possibly with a different geometry to the N-terminal domain of ZntA compared to Zn(II) and Cd(II). The affinity of the N-terminal domain for Zn(II), Pb(II), and Cd(II) was measured using two metallochromic indicators, mag-fura-2 and PAR. N1-ZntA binds these metal ions with association constants of $\sim 10^7-10^8$ M^{-1}.

REFERENCES

1. Axelson, K. B., and Palmgren, M. G. (1998) Evolution of Substrate Specificities in the P-Type ATPase Superfamily, *J. Mol. Evol. 46*, 84−101.
2. Lutsenko, S., and Kaplan, J. H. (1995) Organization of P-type ATPases: Significance of Structural Diversity, *Biochemistry 34*, 15607−15613.
3. Solioz, M., and Vulpe, C. (1996) CPx-type ATPases: a class of P-type ATPases that pump heavy metals, *Trends Biochem. Sci. 21*, 237−241.
4. Rensing C., Mitra B., and Rosen B. P. (1997) The *znt*A gene of *Escherichia coli* encodes a Zn^{2+}-translocating P-type ATPase, *Proc. Natl. Acad. Sci. U.S.A. 94*, 14326−14331.
5. Rensing, C., Sun, Y., Mitra, B., and Rosen, B. P. (1998) Pb^{2+}-translocating P-type ATPases, *J. Biol. Chem. 273*, 32614−32617.
6. Rutherford, J. C., Cavet, J. S., and Robinson, N. (1999) Cobalt-dependent Transcriptional Switching by a Dual-effector MerR-like Protein Regulates a Cobalt-exporting Variant CPx-type ATPase, *J. Biol. Chem. 274*, 25827-25832.
7. Nucifora, G., Chu, L., Misra, T. K., and Silver, S. (1989) Cadmium resistance from *Staphylococcus aureus* plasmid pI258 cadA gene results from a cadmium-efflux ATPase, *Proc. Natl. Acad. Sci. U.S.A. 86*, 3544−3548.
8. Rensing, C., Fan, B., Sharma, R., Mitra, B., and Rosen, B. P. (2000) CopA: an *Escherichia coli* Cu(I)-translocating P-type ATPase, *Proc. Natl. Acad. Sci. U.S.A. 97*, 652−656.
9. Odermatt, A., Suter, H., Krapf, R., and Solioz, M. (1993) Primary Structures of Two P-type ATPases Involved in Copper Resistance in *Enterococcus hirae*, *J. Biol. Chem. 268*, 12775−12779.
10. Mandal, A. K., Cheung, W. D., and Arguello, J. M. (2002) Characterization of a thermophilic P-type Ag^+/Cu^+-ATPase from the extremophile *Archaeoglobus fulgidus*, *J. Biol. Chem. 277*, 7201−7208.
11. Gupta, A., Matsui, K., Lo, J. F., and Silver, S. (1999) Molecular basis for resistance to silver cations in *Salmonella*, *Nat. Med. 5*, 183−188.
12. Bull, P. C., Thomas, G. R., Rommens, J. M., Forbes, J. R., and Cox, D. W. (1993) The Wilson disease gene is a putative copper transporting P-type ATPase similar to the Menkes gene, *Nat. Genet. 5*, 327−337.
13. Vulpe, C., Levinson, B., Whitney, S., Packman, S., and Gitschier, J. (1993) Isolation of a candidate gene for Menkes disease and evidence that it encodes a copper-transporting ATPase, *Nat. Genet. 3*, 7−13.
14. Lutsenko, S., Petrukhin, K., Cooper, M. J., Gilliam, C. T., and Kaplan, J. H. (1997) N-terminal domains of human copper-transporting adenosine triphosphatases (the Wilson's and Menkes disease proteins) bind copper selectively in vivo and in vitro with stoichiometry of one copper per metal-binding repeat, *J. Biol. Chem. 272*, 18939−18944.
15. DiDonato, M., Narindrasorasak, S., Forbes, J. R., Cox, D. W., and Sarkar, B. (1997) Expression, purification, and metal binding properties of the N-terminal domain from the Wilson disease putative copper-transporting ATPase (ATP7B), *J. Biol. Chem. 272*, 33279−33282.
16. Cobine, P. A., George, G. N., Winzor, D. J., Harrison, M. D., Mogahaddas, S., and Dameron, C. T. (2000) Stoichiometry of complex formation between Copper(I) and the N-terminal domain of the Menkes protein, *Biochemistry 39*, 6857−6863.
17. DiDonato, M., Zhang, J., Que, L., Jr., and Sarkar, B. (2002) Zinc binding to the NH_2-terminal domain of the Wilson disease copper-transporting ATPase: implications for in vivo metal ion-mediated regulation of ATPase activity, *J. Biol. Chem. 277*, 13409−13414.
18. Ralle, M., Lutsenko, S., and Blackburn, N. J. (2003) The Menkes Disease Protein Binds Copper via Novel 2-coordinate Cu^+−Cysteinates in the N-Terminal Domain, *J. Biol. Chem. 278*, 23163−23170.
19. Gitschier, J., Moffat, B., Reilly, D., Wood, W. I., and Fairbrother, W. J. (1998) Solution structure of the fourth metal-binding domain from the Menkes copper-transporting ATPase, *Nat. Struct. Biol. 5*, 47−54.
20. Banci, L., Bertini, I., Ciofi-Baffoni, S., Finney, L. A., Outten, C. E., and O'Halloran, T. V. (2002) A new zinc-protein coordination site in intracellular metal trafficking: solution structure of the Apo and Zn(II) forms of ZntA(46−118), *J. Mol. Biol. 323*, 883−897.
21. Mitra, B., and Sharma, R. (2001) The cysteine-rich amino-terminal domain of ZntA, a Pb(II)/Cd(II)/Zn(II)-translocating ATPase from *Escherichia coli*, is not essential for its function, *Biochemistry 40*, 7694−7699.
22. Sharma, R., Rensing, C., Rosen, B. P., and Mitra, B. (2000) The ATP hydrolytic activity of purified ZntA, a $Pb^{2+}/Cd^{2+}/Zn^{2+}$-translocating ATPase from *Escherichia coli*, *J. Biol. Chem. 275*, 3873−3878.
23. Datsenko, K. A., and Wanner, B. L. (2000) One-step inactivation of chromosomal genes in *Escherichia coli* K-12 using PCR products, *Proc. Natl. Acad. Sci. U.S.A. 97*, 6440−6445.
24. Walkup, G. K, and Imperiali, B. (1997) Fluorescent Chemosensors for Divalent Zinc Based on Zinc Finger Domains. Enhanced Oxidative Stability, Metal Binding Affinity, and Structural and Functional Characterization, *J. Am. Chem. Soc. 119*, 3443−3450.
25. Hunt, J. B., Neece, S. H., and Ginsburg A. (1985) The use of 4-(2-pyridylazo)resorcinol in studies of zinc release from *Escherichia coli* aspartate transcarbamoylase, *Anal. Biochem. 146*, 150−157.
26. Riddles, P. W., Blakeley, R. L., and Zerner, B. (1979) Ellman's reagent: 5,5′-dithiobis(2-nitrobenzoic acid)- -a reexamination, *Anal. Biochem. 94*, 75−81.
27. Poole, R. K., Williams, H. D., Downie, J. A., and Gibson, F. (1989) *J. Gen. Microbiol. 135*, 1865−1874.
28. Simons T. J. (1993) Measurement of free Zn^{2+} ion concentration with the fluorescent probe mag-fura-2 (furaptra), *J. Biochem. Biophys. Methods 27*, 25−37.
29. Corsini, A., Yih, I. M.-L., Fernando, Q.; Freiser H. (1962) Potentiometric Investigation of the Metal Complexes of 1-(2-Pyridylazo)-2-naphthol and 4-(2-Pyridylazo)resorcinol, *Anal. Chem. 34*, 1090−1093.
30. Arguello, J. M. (2003) Identification of ion-selectivity determinants in heavy-metal transport P1B-type ATPases, *J. Membr. Biol. 195*, 93−108.
31. Xiao, Z., Loughlin, F., George, G. N., Howlett, G. J. and Wedd, A. G. (2004) C-Terminal Domain of the Membrane Copper Transporter Ctr1 from*Saccharomyces cerevisiae* Binds Four Cu(I) Ions as a Cuprous-Thiolate Polynuclear Cluster: Sub-femtomolar Cu(I) Affinity of Three Proteins Involved in Copper Trafficking, *J. Am. Chem. Soc. 126*, 3081−3090.

BI0476275